Preprint Title A numerical modeling of a multi-frequency receiving system based on an array of dipole antennas with cold-electron bolometers for LSPE-SWIPE

Authors Alexander V. Chiginev, Anton V. Blagodatkin, Dmitrii A. Pimanov, Ekaterina A. Matrozova, Anna V. Gordeeva, Andrey L. Pankratov and Leonid S. Kuzmin

Publication Date 27 Jun 2022

Article Type Full Research Paper

ORCID® iDs Anton V. Blagodatkin - https://orcid.org/0000-0002-0025-4970; Dmitrii A. Pimanov - https://orcid.org/0000-0002-5323-5642; Ekaterina A. Matrozova - https://orcid.org/0000-0003-1013-1365; Andrey L. Pankratov - https://orcid.org/0000-0003-2661-2745

A numerical modeling of a multi-frequency receiving system based on an array of dipole antennas with cold-electron bolometers for LSPE-SWIPE

A. V. Chiginev[1,2,*], A. V. Blagodatkin[1], D. A. Pimanov[1,3], E. A. Matrozova[1], A. V. Gordeeva[1,2], A. L. Pankratov[1,2] and L. S. Kuzmin[1,3]

Address: [1]Nizhny Novgorod State Technical University, Nizhny Novgorod, Minin Street, 24, 603950, Russia, [2]Institute for Physics of Microstructures of the Russian Academy of Sciences, GSP-105, Nizhny Novgorod, 603950, Russia and [3]Chalmers University of Technology, Department of Microtechnology and Nanoscience - MC2, Gothenburg, SE-412 96, Sweden

Email: Alexander V. Chiginev – chig@ipmras.ru

Abstract

We present the results of numerical modeling of mode composition in the constriction of the LSPE-SWIPE back-to-back horn. These results are used for calculating the frequency response of arrays of planar dipole antennas with cold-electron bolometers for frequencies 145, 210 and 240 GHz. For the main frequency channel, 145 GHz, we have 45 GHz bandwidth. For the auxiliary frequency channels, 210 and 240 GHz, placed on the same substrate, we have 26 GHz and 38 GHz bandwidth, correspondingly. We have performed some optimizations for cold-electron bolometers to achieve photon NEP at the level of 1.1×10^{-16} W/Hz$^{1/2}$. This was achieved by replacing one of two SIN tunnel junctions with the SN contact.

Keywords

cold-electron bolometer; CMB; dipole antenna; waveguide horn; dichroic antenna

Introduction

The Large Scale Polarization Explorer (LSPE) [1] is an experiment of the Italian Space Agency for observing the polarization pattern of the B-mode of the cosmic microwave background (CMB). These observations can give an important information about primordial gravitational waves. LSPE project consists of two instruments: Strip and Short-Wavelength Instrument for the Polarization Explorer (SWIPE). LSPE-SWIPE is a balloon-borne radio telescope, it will consist of the main and two auxiliary frequency channels. According to the latest requirements [2], the operating frequency of the LSPE-SWIPE main frequency channel should be 145 GHz with a bandwidth of 30%. The operating frequencies of the auxiliary channels should be equal to 210 and 240 GHz, the bandwidths should be 20% and 10%, respectively. To receive radiation in the indicated frequency ranges, we propose to use arrays of planar dipole antennas located in the opening of a special bidirectional horn that forms the radiation pattern of the receiving system and also serves as a low-frequency filter.

For radiation detection, many bolometer types can be applied. The detectors for this instrument should work at 300 mK, because it is the working temperature of the ^{3}He cryostat used for LSPE project. One of main candidates for LSPE-SWIPE is transition-edge sensor (TES) with a spider-web antenna [2, 3]. For OLIMPO mission, kinetic inductance detectors (KIDs) were used [4]. We propose to use cold-electron bolometers (CEBs) [5, 6] integrated into dipole antennas. The advantages of CEB over other types of bolometers are, in particular, their high sensitivity with background-limited operation [6-8] and wide dynamic range. These qualities are

largely determined by the presence of internal self-cooling of the electronic subsystem of the CEB absorber [6-8]. Another key advantage for balloon and space missions is the high immunity of CEB to Cosmic Rays [9] due to double protection by extremly small volume of absorber and decoupling of electron and phonon systems.

One of the advantages of our implementation is the possibility to make arrays for two auxiliary channels 210 and 240 GHz on the same pixel because of small size of CEBs. The use of multichroic pixels increases the number of pixels per frequency, at no extra cost per focal plane area, weight and cryogenic load. Before, the double-frequency system with slot antennas and CEBs for frequencies 75 and 105 GHz for Cosmic Origins Explorer (COrE) mission has been investigated and band separation was demonstrated [10]. Now this approach is getting further improvements with arrays of dipole antennas and voltage-biased mode. To use this mode, the CEBs must be connected in parallel. SQUIDs with multiplexing [11] will be used for readout. Therefore, to match this readout system, the arrays of dipole antennas and CEBs connected in parallel should have resistance of 1 Ohm at the working point.

In the present paper, we describe the problems of numerical modeling for double-frequency arrays of dipole antennas connected in parallel on a single substrate with radiation going through the back-to-back horn with predefined parameters.

Results

Calculation of the mode composition in the constriction of the horn at the incidence of a plane linearly polarized wave

The parameters of the back-to-back horn are defined in [3]. It consists of two openings and a constriction connecting them, see the details in [3] and a part of the horn below in Figure 1. One of the openings defines the radiation pattern of the

receiving system, and the other is facing the receiving antenna array. The constriction of the horn determines the modal composition of the electromagnetic field passing through the horn. For a given constriction diameter, up to 38 modes of a circular waveguide are propagating in the operating frequency range.

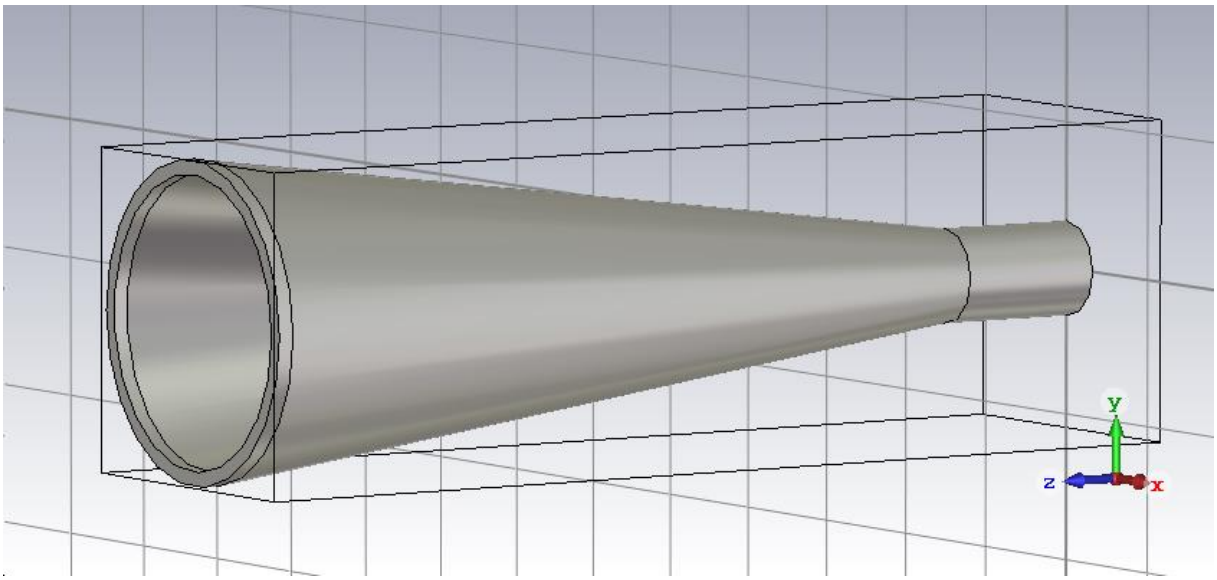

Figure 1: The front part and the constriction of the back-to-back horn of the LSPE-SWIPE receiving system [3], used for the calculation of the mode composition in the constriction.

For correct numerical modeling of the frequency response of the receiving system, it is necessary to know the distribution of the field of the wave incident on the matrix of receiving cells. The most consistent would be modeling a back-to-back horn irradiated by a plane electromagnetic wave with a receiving matrix installed in the opposite opening. However, this task requires a lot of computational resources. Therefore, the problem of irradiating the receiving matrix with incoming radiation was divided into two parts. The first problem is to determine the mode composition of radiation passing through the constriction of a back-to-back horn when a plane electromagnetic wave falls on it (Figure 1). The second problem is to calculate the

power absorbed by the receiving matrix when this matrix is irradiated by the electromagnetic field of a round waveguide port with the calculated mode composition.

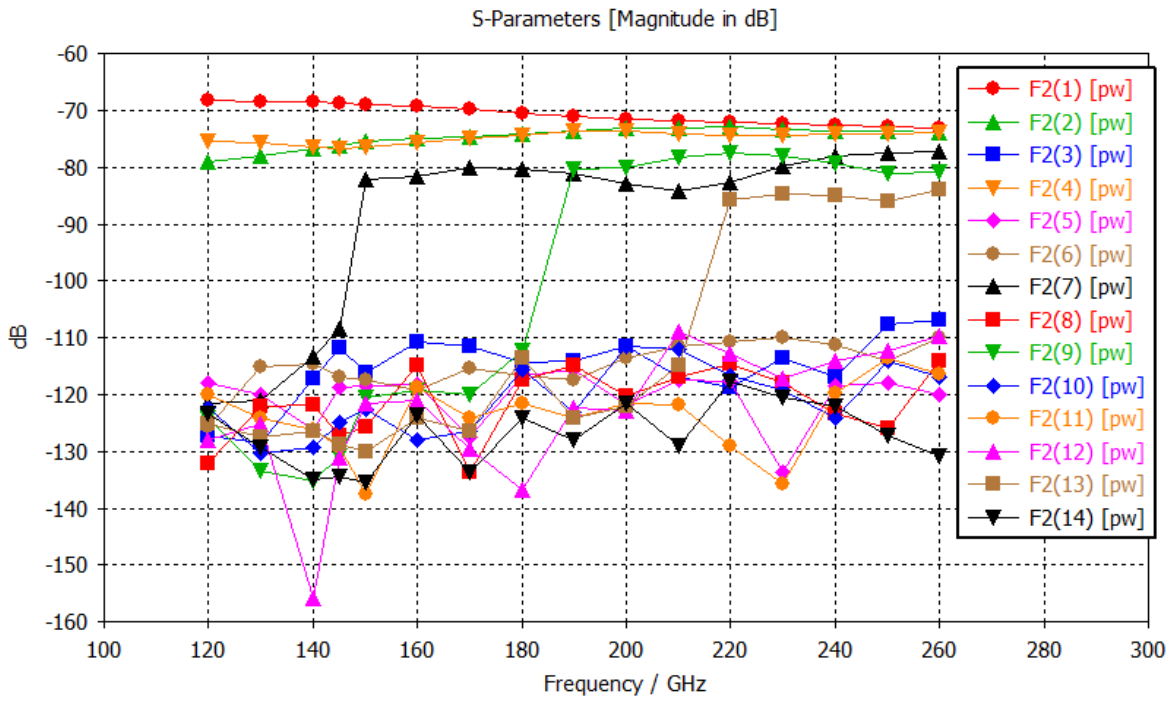

Figure 2: The mode composition of the electromagnetic field in the constriction of a bidirectional horn as a function of frequency.

The result of the calculation of the mode composition in a back-to-back horn is shown in Figure 2. It can be seen that over the entire operating frequency range of LSPE-SWIPE, modes with numbers 1 (main), 2 and 4 are present in the horn. Starting from the frequency of 150 GHz, mode 7 appears; amplitudes of modes 7, 9, 13 are associated with the achievement of the corresponding cut-off frequencies of these modes. The amplitudes of the remaining modes are negligible compared to the amplitudes of the listed modes, so they can be ignored in what follows. The calculated mode amplitudes will be used in calculating the frequency response of

antenna arrays with integrated bolometers for the main and auxiliary frequency channels of LSPE-SWIPE.

Calculation of frequency response of planar antenna matrix with integrated CEBs

The frequency response of the receiving matrix was calculated as follows. The radiation incident on the matrix is formed by the waveguide port of a circular waveguide with a diameter corresponding to the wide part of the bidirectional horn facing the receiving system (on the right in Figure 1). An RC circuit was used as an equivalent circuit for CEB at high frequencies. In the process of numerical simulation, we calculated the dependence of the power P_{i}, released on the active resistance of the i-th RC-chain of the array of receiving cells, on the frequency of the incident radiation, and the total power in all receiving cells

$$P(f) = \sum_{i=1}^{N} P_i(f) \quad (1)$$

The summation was performed over the cells included in one frequency channel. Thus, as a result of the calculation, the frequency response of the receiving system of one frequency channel was obtained. This calculation principle was used for all types of the receiving matrix of the LSPE-SWIPE auxiliary frequency channels.

Main frequency channel of LSPE-SWIPE

The LSPE-SWIPE 145 GHz main channel receiving system is based on an array of dipole antennas with integrated CEBs (Figure 3). The receiving cells are located within a circle, under the opening of a bidirectional horn. Its characteristic feature is that the antenna dipoles and wires that provide the CEB DC bias are located in the same layer. This significantly simplifies and reduces the cost of manufacturing such structures.

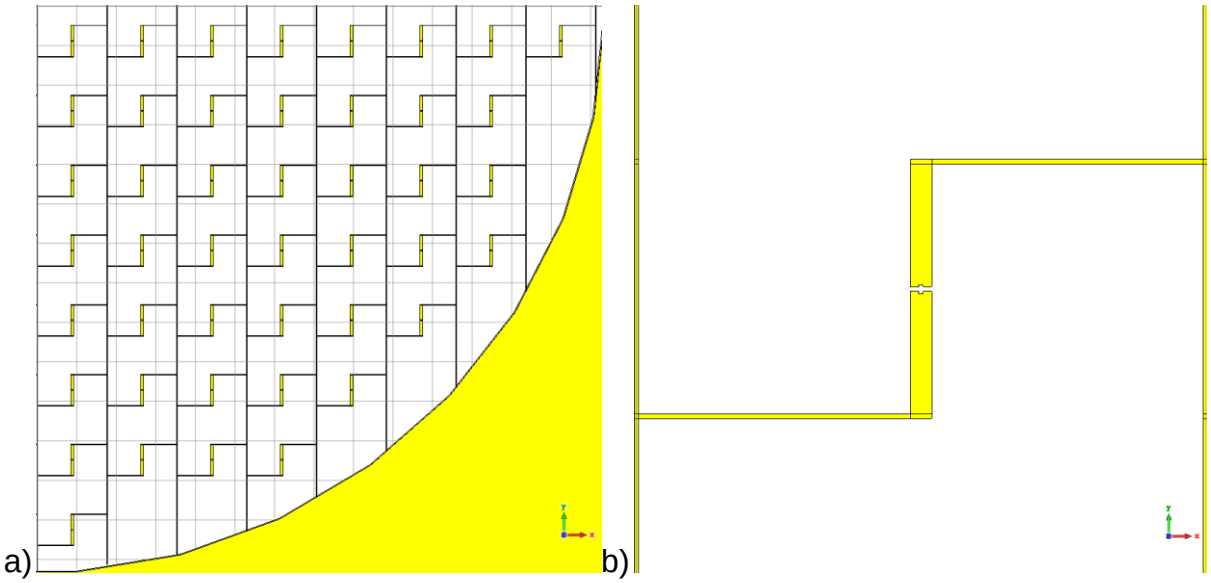

Figure 3: Receiving system of the 145 GHz main channel of LSPE-SWIPE. a) A quarter of receiving cells matrix on the 14 mm chip; b) single cell of the receiving system based on a dipole antenna.

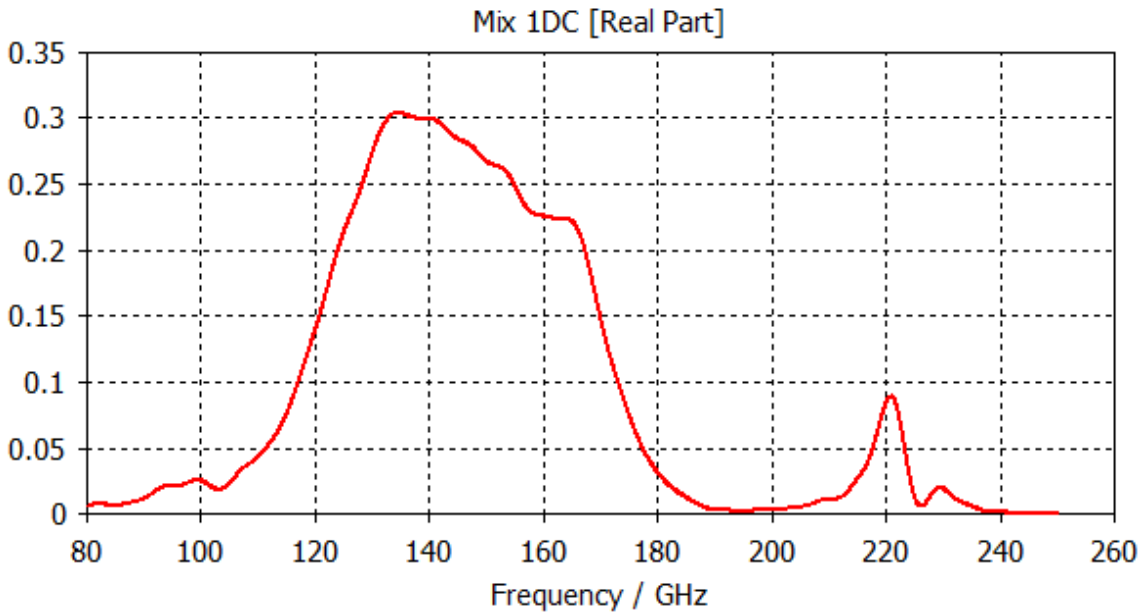

Figure 4: Frequency response of the LSPE-SWIPE 145 GHz main frequency channel.

The frequency response of the LSPE-SWIPE 145 GHz main frequency channel is shown in Figure 4. The received frequency band of the main frequency channel at the level of 0.5 is 45 GHz. At 220 GHz there is a spurious resonance that can be suppressed with a low-pass filter.

Auxiliary frequency channels of LSPE-SWIPE

The cells are located within a circle with a diameter of 4.5 mm, while one half of the circle is occupied by cells for 210 GHz, and the second half by cells for 240 GHz. Receiving cells with integrated CEBs are located on a 260 μm thick silicon substrate with silicon dioxide layer. The difficulty of the considered receiving system is the existing specific sample holder, allowing the receiving of the signal from the front side of the pixel only with the back-short placed at the back side of the pixel. Such configuration leads to more tough constraints and less number of free parameters than in [10], where the signal was coming to the antennas through the substrate.

In the work, the receiving system based on a bow-tie dipole antenna was calculated (Figure 5) with the DC bias lines connected to the central parts of antennas.

a) 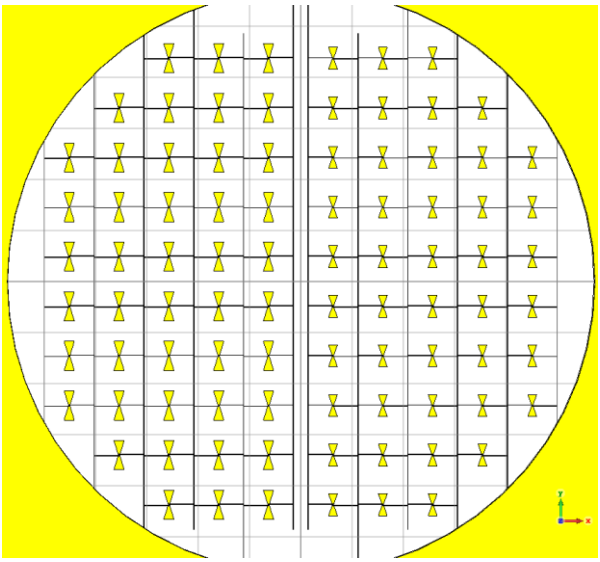 b) 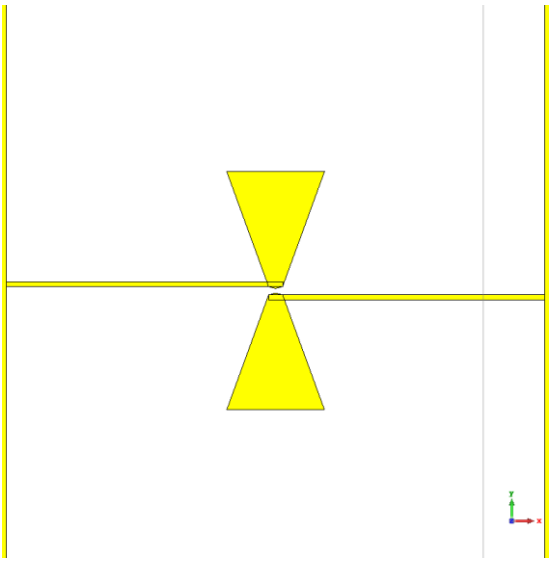

Figure 5: a) Receiving cell array based on bow-tie antennas, with a half of the 7 mm plate at the left are 210 GHz and at the right – 240 GHz frequency channels; b) a receiving system cell based on a bow-tie antenna.

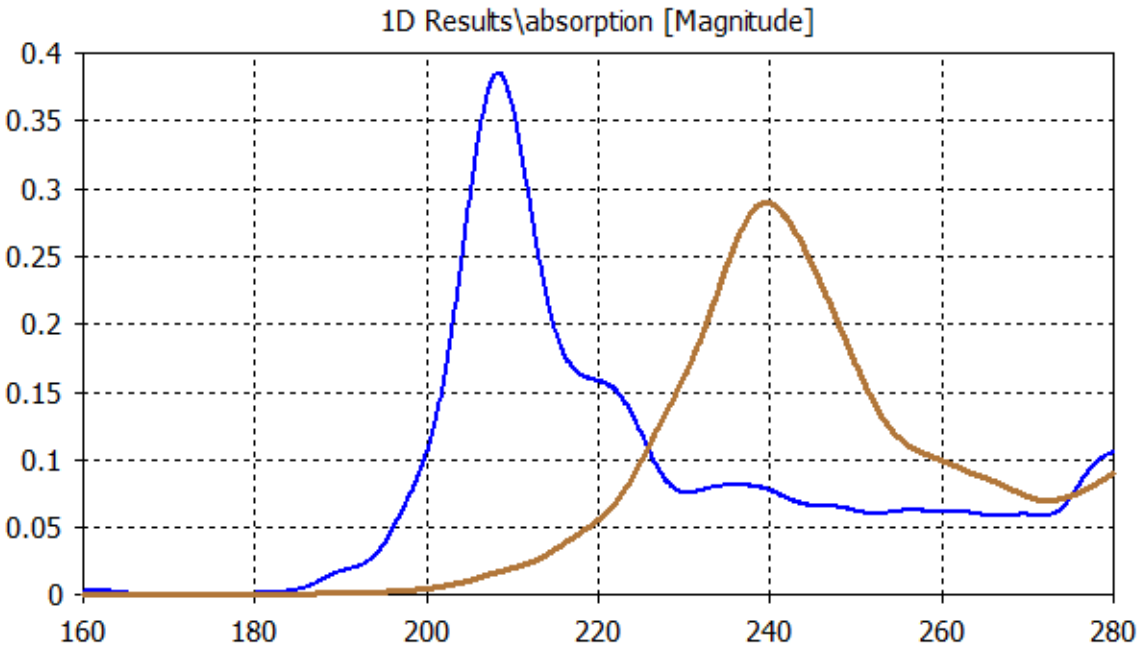

Figure 6: Frequency response of a matrix of receiving cells based on bow-tie antennas for 210 GHz and 240 GHz frequency channels.

The frequency response of the receiving matrix with bow-tie antennas is shown in Figure 6. Rather good band separation is visible in spite of a certain cross-talk of 210 GHz channel. The frequency response width at the level of 50% of the maximum for the 210 GHz channel is 26 GHz, for the 240 GHz channel – 38 GHz. In addition, the RF tails of the 240 GHz channel above 270 GHz are supposed to be suppressed by a band-pass filter.

NEP calculations for LSPE-SWIPE

The power load for the LSPE-SWIPE 145, 210 and 240 GHz frequency channels should be 11, 12.4 and 16 pW, respectively, as stated in Table 4 in [2]. The total NEP level should be about 7×10^{-17} W/Hz$^{1/2}$ for 145 GHz channel, 8.5×10^{-17} W/Hz$^{1/2}$ for 210 GHz channel and 1.3×10^{-16} W/Hz$^{1/2}$ for 240 GHz channel at the working point for background (photon-noise) limited operation. However, the readout system is based on SQUIDs, and this system has input current noise at the level of 4-10 pA/Hz$^{1/2}$. To optimize the receiver for better noise characteristics, we consider optimized CEBs with a single SIN tunnel junction and a single SN contact [12]. Combined together, they form a SINS structure.

This solution can help reaching better noise characteristics than CEBs with two SIN tunnel junctions due to several reasons. First, the responsivity is increased by a factor of two due to hot electrons tunnelling only through one SIN junction. Second, the bolometer resistance is decreased twice, which helps in array matching with a SQUID readout (we remind here that the total resistance of this array should be 1 Ohm). Third, the electron cooling efficiency is increased by a factor of two due to readout current increased twice for the same power going through the system. And the last, but not the least, the absence of the second SIN tunnel junction suppresses the Coulomb blockade, so the absorber volume can be decreased by a factor of four, leaving the capacitance the same.

Therefore, the current responsivity is increased from 40-45 nA/pW to 80-100 nA/pW. So the total NEP for this CEB concept should be also twice better than the total NEP for CEBs with two SIN tunnel junctions and it should be close to the required photon NEP level for the LSPE-SWIPE frequency channels. This comparison for arrays of 66 SINS CEBs with 6 pW power load is shown in Figure 2 in [12].

For better NEP estimation we should also account for the matching of CEBs array with the SQUID readout system. The mismatching can happen if we have dynamic resistance of the CEBs array at the working point with the parasitic resistance of connecting wires more than 1 Ohm. Then the noise of the SQUID readout system is getting multiplied on the square root of the ratio of the obtained dynamic resistance of the CEBs array and the connecting wires to the required value of 1 Ohm. NEP estimations for different numbers of CEBs in a parallel array for 145, 210 and 240 GHz frequency channels with the account of possible mismatching with the SQUID readout system are shown below with SQUID noise of 10 pA/Hz$^{1/2}$.

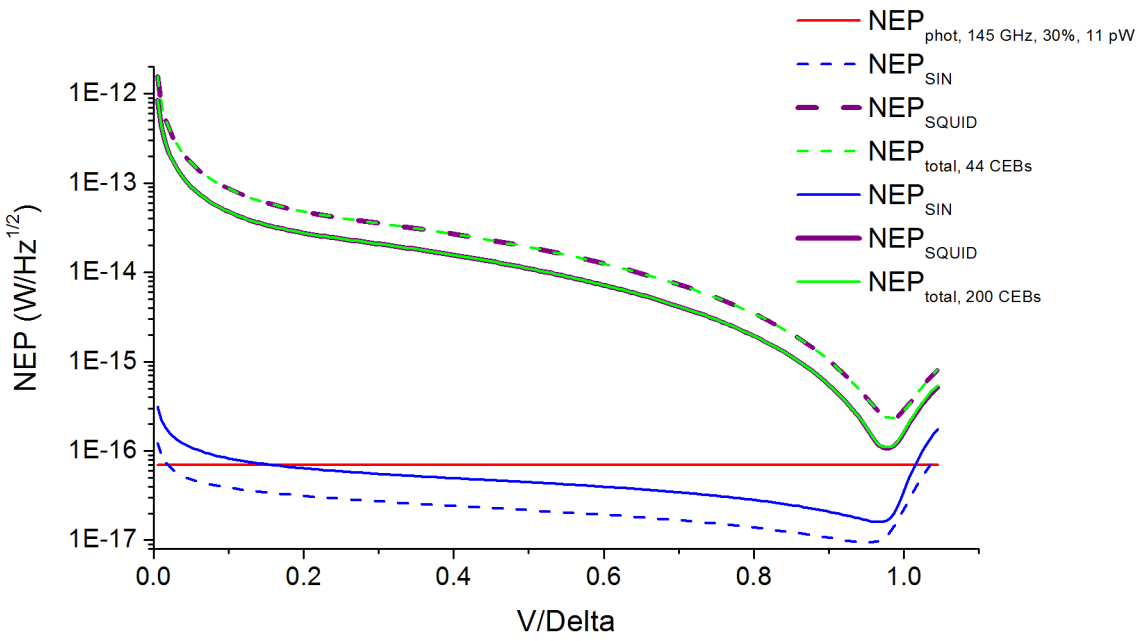

Figure 7: NEP estimations for 145 GHz channel with 11 pW power load. Dashed curves are for 44 SINS CEBs; solid curves are for 200 SINS CEBs.

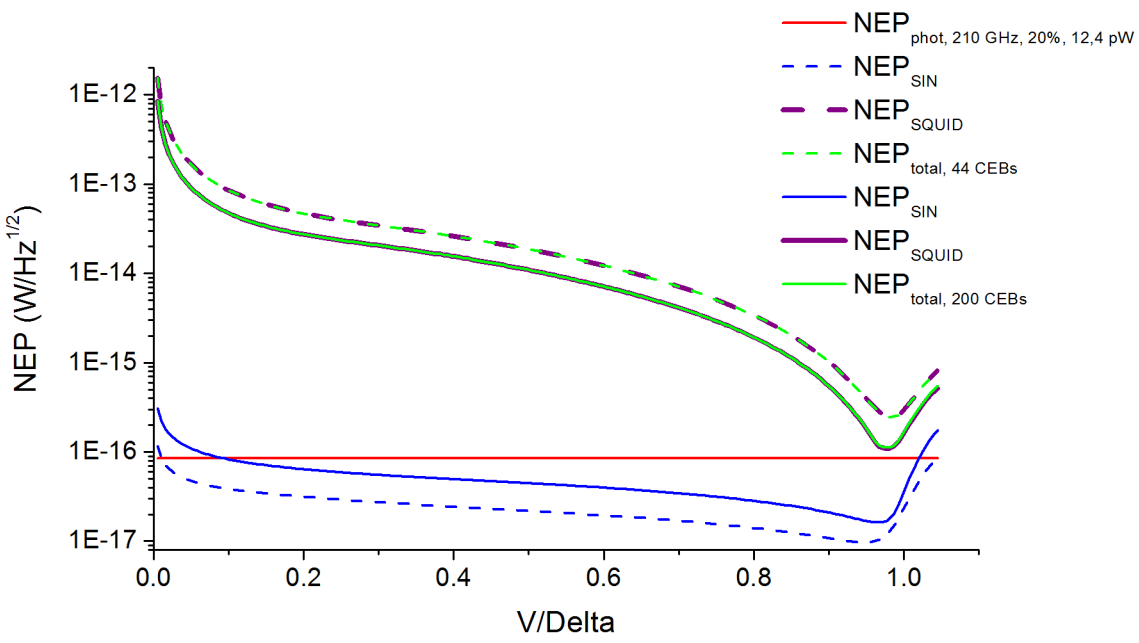

Figure 8: NEP estimations for 210 GHz channel with 12.4 pW power load. Dashed curves are for 44 SINS CEBs; solid curves are for 200 SINS CEBs.

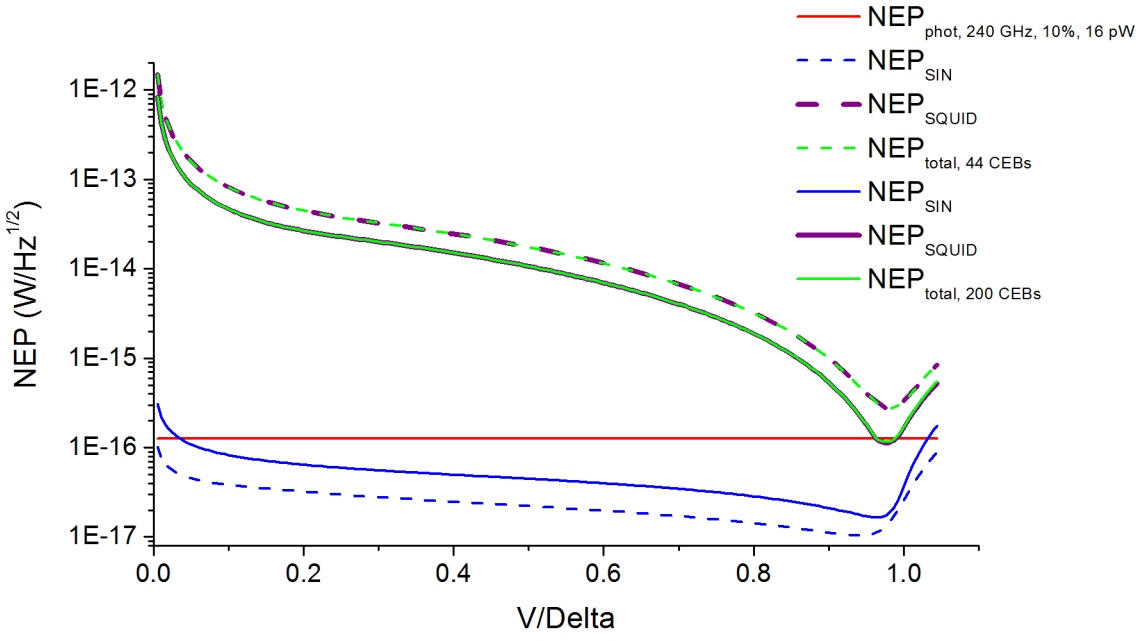

Figure 9: NEP estimations for 240 GHz channel with 16 pW power load. Dashed curves are for 44 SINS CEBs; solid curves are for 200 SINS CEBs.

In Figure 7 and Figure 8 it is seen that the total NEP level (green curves), which includes the NEP of SIN junctions (blue curves) and the NEP of SQUID readout system (purple curves), nearly approaches the photon NEP level (red line), so the increase of CEBs number improves the total NEP. For 200 SINS CEBs of 240 GHz frequency channel (Figure 9, solid curves) the total NEP curve reaches the photon NEP line at the working point. The minimal value of total NEP in this case is 1.15×10^{-16} W/Hz$^{1/2}$.

These estimations were calculated for input current noise of SQUID readout system at the pessimistic level of 10 pA/Hz$^{1/2}$. If this noise is reduced twice, to 5 pA/Hz$^{1/2}$, the minimal value of the total NEP for 200 SINS CEBs of 240 GHz frequency channel falls below to 7×10^{-17} W/Hz$^{1/2}$. In addition, photon-noise limit can be easily reached for all frequency channels with the use of the Quasiparticle Cascade Amplifier (QCA), which can be added to the SINS CEB. The great benefits of using the QCA are described in detail in [12].

Conclusion

The calculation of the mode composition in the constriction of the LSPE-SWIPE back-to-back horn helps us in modeling the frequency response of the receiving systems. We use the calculated mode amplitudes for calculating the frequency response of the arrays of dipole antennas for all frequency channels of LSPE-SWIPE receiving system.

We have developed the arrays of dipole antennas which can be applicable for all frequency channels of LSPE-SWIPE. For this purpose we have used both the straight dipole antennas and the bow-tie shaped dipole antennas, which are very useful for meeting the bandwidth requirements for different frequency channels.

To achieve NEP level for photon-noise limited operations, we have performed a very important optimization for cold-electron bolometer design. We changed one of two SIN tunnel junctions to the SN contact, so now it is a SINS structure. This change allowed us to increase current responsivity twice and to improve total NEP by the same factor. However, further improvements can be achieved by the use of the Quasiparticle Cascade Amplifier [12].

Funding

This work has been supported by Russian Science Foundation (Grant #21-79-20227).

References

1. Aiola, S. et al. *Proc. SPIE,* **2012,** *V. 8446,* 84467A.
2. The LSPE collaboration et al. *J. Cosmol. Astropart. Phys.,* **2021,** *V. 2021, Issue 8,* 008.
3. Lamagna, L. et al. *J. Low Temp. Phys.,* **2020,** *V. 200, Issue 5-6,* 374–383.
4. Masi, S. et al. *J. Cosmol. Astropart. Phys.,* **2019,** *V. 2019, Issue 7,* 003.
5. Kuzmin, L. S. *In International Workshop on Superconducting Nano-Electronics Devices,* **2002,** 145–154.
6. Kuzmin, L. S., Pankratov, A. L., Gordeeva, A. V., Zbrozhek, V. O., Shamporov, V. A., Revin, L. S., Blagodatkin, A. V., Masi, S., de Bernardis, P. *Commun. Phys.,* **2019,** *V. 2,* 104.
7. Gordeeva, A. V., Zbrozhek, V. O., Pankratov, A. L., Revin, L. S., Shamporov, V. A., Gunbina, A. A., Kuzmin, L. S. *Appl. Phys. Lett.,* **2017**, *V. 110*, 162603.

8. Gordeeva, A. V., Pankratov, A. L., Pugach, N. G., Vasenko, A. S., Zbrozhek, V. O., Blagodatkin, A. V., Pimanov, D. A., Kuzmin, L.S. *Sci. Rep.,* **2020,** *V. 10,* 21961.
9. Salatino, M., de Bernardis, P., Kuzmin, L., Mahashabde, S., Masi, S. *J. Low Temp. Phys.*, **2014**, *V. 176*, 323–330.
10. Kuzmin, L. S., Blagodatkin, A. V., Mukhin, A. S., Pimanov, D. A., Zbrozhek, V. O., Gordeeva, A. V., Pankratov, A. L., Chiginev, A. V. *Supercond. Sci. Technol.,* **2019,** *V. 32,* 035009.
11. Heinz, E., Zakosarenko, V., May T., Meyer, H.G. *Supercond. Sci. Technol.,* **2013,** *V. 26,* 045013.
12. Kuzmin, L. S., Golubev, D. S. *IEEE Trans. Appl. Supercond.*, **2022,** *V. 32, No. 4,* 2300205.